Inorganic Chemistry
Article

Inorg. Chem. **2010**, *49*, 1027–1038 **1027**
DOI: 10.1021/ic901851u

Electrochemistry and Spectroelectrochemistry of β,β′-Fused Quinoxalinoporphyrins and Related Extended Bis-porphyrins with Co(III), Co(II), and Co(I) Central Metal Ions

Weihua Zhu,[†,§] Maxine Sintic,[‡] Zhongping Ou,*[,†,§] Paul J. Sintic,[‡] James A. McDonald,[‡] Peter R. Brotherhood,[‡] Maxwell J. Crossley,*[,‡] and Karl M. Kadish*[,†]

[†]*Department of Chemistry, University of Houston, Houston, Texas 77204-5003,* [‡]*School of Chemistry, The University of Sydney, NSW 2006, Australia, and* [§]*Department of Applied Chemistry, Jiangsu University, Zhenjiang, 212013, China*

Received September 18, 2009

A series of cobalt(II) and cobalt(III) porphyrins with fused quinoxaline rings at one or more β,β′-pyrrolic units of the macrocycle were synthesized and characterized as to their electrochemical properties in nonaqueous media. Their UV−visible spectra were also measured before and during oxidation or reduction in a thin-layer cell. The investigated quinoxalinoporphyrins are represented as (PQ)Co, (QPQ)CoCl, (PQ_2)CoCl, Co(P)-TA-(P)Co, and Co(PQ)-(QP)Co, where PQ = the dianion of 5,10,15,20-tetrakis(3,5-di-*tert*-butylphenyl)-quinoxalino[2,3-*b*′]porphyrin, QPQ = the dianion of the corresponding linear bisquinoxalino[2,3-*b*′:12,13-*b*′′]porphyrin, PQ_2 = the dianion of the corresponding corner bisquinoxalino[2,3-*b*′:7,8-*b*′′]porphyrin, and (P)-TA-(P) = the tetraanion of the bis-porphyrin with 5,10,15,20-tetrakis-(3,5-di-*tert*-butylphenyl)porphyrins fused at opposite ends of tetraazaanthracene. (P)Co and (P)CoCl were also characterized where P = the dianion of 5,10,15,20-tetrakis(3,5-di-*tert*-butylphenyl)porphyrin. Each compound could be cycled between their Co(III), Co(II), and Co(I) forms under the application of a given oxidizing or reducing potential, although a one-electron reduction of the Co(II) quinoxalinoporphyrins led to a product with mixed Co(I) and porphyrin π-anion radical character followed by generation of a pure Co(I) π-anion radical species at more negative potentials. The effect of the position and number of quinoxaline groups on the redox potentials and mechanisms of each electron transfer were elucidated, and comparisons made to structurally similar compounds containing both redox active and redox inactive central metal ions. Surprisingly, the position and number of quinoxaline groups on the macrocycle has little or no effect on the redox potentials for the Co(II) → Co(III) or Co(III) → Co(II) processes, but this is not the case for other electron transfer reactions where significant differences are seen between the examined compounds. Significant interactions are also observed between the two porphyrin macrocycles of the laterally bridged dicobalt(II) bis-porphyrin dyad Co(P)-TA-(P)Co in its singly and doubly reduced form, but only weak interactions are seen between the two Co(PQ) units of the single bond biquinolalinyl-bridged dicobalt(II) bis-porphyrin dyad Co(PQ)-(QP)Co.

Introduction

Numerous quinoxalinoporphyrins have been electrochemically examined in recent years[1−14] as models for the development of porphyrin-based molecular wires and devices.[4,6,10,15−18] Fusion of one or more quinoxaline groups to the β,β′-pyrrolic units of 5,10,15,20-tetrakis(3,5-di-*tert*-butylphenyl)porphyrin has only a minimal effect on the

*To whom correspondence should be addressed. E-mail: kkadish@uh.edu.

(1) Hutchison, J. A.; Sintic, P. J.; Brotherhood, P. R.; Scholes, C.; Blake, I. M.; Ghiggino, K. P.; Crossley, M. J. *J. Phys. Chem. C* **2009**, *113*, 11796–11804.
(2) Hutchison, J. A.; Sintic, P. J.; Crossley, M. J.; Nagamura, T.; Ghiggino, K. P. *Phys. Chem. Chem. Phys.* **2009**, *11*, 3478–3489.
(3) Fukuzumi, S.; Ohkubo, K.; Zhu, W.; Sintic, M.; Khoury, T.; Sintic, P. J.; E, W.; Ou, Z.; Crossley, M. J.; Kadish, K. M. *J. Am. Chem. Soc.* **2008**, *130*, 9451–9458.
(4) Sintic, P. J.; E, W.; Ou, Z.; Shao, J.; McDonald, J. A.; Cai, Z.-L.; Kadish, K. M.; Crossley, M. J.; Reimers, J. R. *Phys. Chem. Chem. Phys.* **2008**, *10*, 268–280.
(5) Ou, Z.; E, W.; Zhu, W.; Thordarson, P.; Sintic, P. J.; Crossley, M. J.; Kadish, K. M. *Inorg. Chem.* **2007**, *46*, 10840–10849.
(6) Armstrong, R. S.; Foran, G. J.; Hough, W. A.; D'Alessandro, D. M.; Lay, P. A.; Crossley, M. J. *Dalton Trans.* **2006**, 4805–4813.
(7) Ohkubo, K.; Sintic, P. J.; Tkachenko, N. V.; Lemmetyinen, H.; E, W.; Ou, Z.; Shao, J.; Kadish, K. M.; Crossley, M. J.; Fukuzumi, S. *Chem. Phys.* **2006**, *326*, 3–14.
(8) Ou, Z.; E, W.; Shao, J.; Burn, P. L.; Sheehan, C. S.; Walton, R.; Kadish, K. M.; Crossley, M. J. *J. Porphyrins and Phthalocyanines* **2005**, *9*, 142–151.
(9) Ou, Z.; Kadish, K. M.; E, W.; Shao, J.; Sintic, P. J.; Ohkubo, K.; Fukuzumi, S.; Crossley, M. J. *Inorg. Chem.* **2004**, *43*, 2078–2086.
(10) Crossley, M. J.; Sintic, P. J.; Walton, R.; Reimers, J. R. *Org. Biomol. Chem.* **2003**, *1*, 2777–2787.
(11) Crossley, M. J.; Johnston, L. A. *Chem. Commun.* **2002**, 1122–1123.
(12) Kadish, K. M.; E, W.; Ou, Z.; Shao, J.; Sintic, P. J.; Ohkubo, K.; Fukuzumi, S.; Crossley, M. J. *Chem. Commun.* **2002**, 356–357.
(13) Fukuzumi, S.; Ohkubo, K.; E, W.; Ou, Z.; Shao, J.; Kadish, K. M.; Hutchison, J. A.; Ghiggino, K. P.; Sintic, P. J.; Crossley, M. J. *J. Am. Chem. Soc.* **2003**, *125*, 14984–14985.
(14) E, W.; Kadish, K. M.; Sintic, P. J.; Khoury, T.; Govenlock, L. J.; Ou, Z.; Shao, J.; Ohkubo, K.; Reimers, J. R.; Fukuzumi, S.; Crossley, M. J. *J. Phys. Chem. A* **2008**, *112*, 556–570.

Published on Web 12/22/2009

oxidation potentials,[3−5,8,9] and this contrasts with the reductions which are positively shifted in potential by 90−190 mV per each fused quinoxaline group, with the exact magnitude of the shift depending upon the solvent, type, and oxidation state of the central metal ion and number of fused quinoxaline groups on the porphyrin macrocycle which can vary from 1 to 4.[19] The site of electron transfer in free-base quinoxalinoporphyrins and quinoxalinoporphyrins containing non-redox active transition metal ions involves primarily the conjugated π-ring system of the porphyrin macrocycle but partial electron density is located on the quinoxaline part of the molecule after reduction,[3,4,8] especially in solutions containing added protons[5] or scandium(III) ion,[20] both of which will bind or ion pair with the quinoxaline nitrogen atoms.

Understanding the most important factors which affect the site of electron transfer in quinoxalinoporphyrins is of vital interest to tune and direct the chemical reactivity of larger arrays containing the quinoxalinoporphyrin unit.[10] This is especially true in the case of redox active transition metal derivatives where the porphyrin central metal ion can be stepwise cycled between its M^{I}, M^{II}, M^{III} or even M^{IV} and M^{V} forms as a function of the applied potential and variations in the type and number of axial ligands.[15] It is well-documented in the literature that the site of electron transfer in metalloporphyrins can be tuned by appropriate selection of solvent, axial ligand binding, and/or porphyrin ring substituents,[9,21,22] and this should also be the case for quinoxalinoporphyrins which have been synthesized to function as integral parts of molecular wires.[15−18]

Our laboratories have studied in detail the redox reactivity of (P)M, (PQ), (QPQ)M, and (PQ_2)M in their neutral, oxidized, and reduced forms where PQ = the dianion of 5,10,15,20-tetrakis(3,5-di-*tert*-butylphenyl)quinoxalino[2,3-*b*′]porphyrin, QPQ = the dianion of the corresonding linear bisquinoxalino[2,3-*b*′:12,13-*b*″]porphyrin, PQ_2 = the dianion of the corresponding corner bisquinoxalino[2,3-*b*′:7,8-*b*″]porphyrin, and M = Zn(II), Ni(II), Cu(II), or Pd(II). The ease of reductions follows the order: (P)M < (PQ)M < (QPQ)M with the difference in $E_{1/2}$ being 160−170 mV between (P)M and (PQ)M or (PQ)M and (QPQ)M, independent of the central metal ion.[5,8] A linear correlation is thus seen between $E_{1/2}$ of the first reduction and the number of fused quinoxaline groups on the macrocycle for these three series of compounds. The (PQ_2)M derivatives do not fit the trend since the π-system of both Q groups are not fully conjugated with the porphyrin macrocycle.[14]

A similar linear relationship is observed for the reduction of Ag(II) porphyrins with P, PQ, or QPQ macrocycles despite the fact that these compounds undergo a metal-centered Ag^{II}/Ag^{I} process[3] as opposed to ring-centered reduction for the other investigated compounds. The site of electron transfer should be important in evaluating the redox behavior of quinoxalinoporphyrins, but the oxidation state of the central metal ion in the initial compounds should also be considered. We earlier examined Au(III) and Au(II) quinoxalinoporphyrins[9,12] and now turn our attention to the cobalt derivatives which can exist in Co(III), Co(II), and Co(I) oxidation states under the appropriate application of an oxidizing or reducing potential. Numerous synthetic cobalt porphyrins with a variety of meso and β-pyrrolic substituents have been studied as to their spectroscopic and electrochemical properties under different solution conditions,[21−40] but cobalt quinoxalinoporphyrins have never before been characterized.

The site of reduction or oxidation in cobalt quinoxalinoporphyrins can, in principle, involve the cobalt central metal ion, the conjugated π-ring system of the porphyrin macrocycle, or the quinoxaline part of the molecule, all of which are redox active.[3,8,21] This is examined in the present study where seven new compounds were synthesized and characterized as to their electrochemical and spectroscopic properties after oxidation and reduction in PhCN containing 0.1 M tetra-*n*-butylammonium perchlorate (TBAP). The examined compounds are shown in Chart 1 and represented as (P)Co, (P)CoCl, (PQ)Co, (QPQ)CoCl, (PQ_2)CoCl, Co(P)-TA-(P)-Co, and Co(PQ)-(QP)Co, where TA = tetraazaanthracene. The magnitude of electronic coupling between the two porphyrin macrocycles of a laterally bridged dicobalt(II) bis-porphyrin dyad, Co(P)-TA-(P)Co **6** and the single bond biquinolalinyl-bridged dicobalt(II) bis-porphyrin dyad dyad, Co(PQ)-(QP)Co **7**, are also explored.

Experimental Section

Instrumentation. Melting points were recorded on a Reichert melting point stage and are uncorrected. Microanalyses were performed at the Microanalytical Unit, The University of New

(15) Sendt, K.; Johnston, L. A.; Hough, W. A.; Crossley, M. J.; Hush, N. S.; Reimers, J. R. *J. Am. Chem. Soc.* **2002**, *124*, 9299–9309.
(16) Reimers, J. R.; Hall, L. E.; Crossley, M. J.; Hush, N. S. *J. Phys. Chem. A* **1999**, *103*, 4385–4397.
(17) Hush, N. S.; Reimers, J. R.; Hall, L. E.; Johnston, L. A.; Crossley, M. J. *Ann. N.Y. Acad. Sci.* **1998**, *852*, 1–21.
(18) Lu, T. X.; Reimers, J. R.; Crossley, M. J.; Hush, N. S. *J. Phys. Chem.* **1994**, *98*, 11878–84.
(19) Khoury, T.; Crossley, M. J. *New J. Chem.* **2009**, *33*, 1076–1086.
(20) Ohkubo, K.; Garcia, R.; Sintic, P. J.; Khoury, T.; Crossley, M. J.; Kadish, K. M.; Fukuzumi, S. *Chem. Eur. J.* **2009**, *15*, 10493−10503.
(21) Kadish, K. M.; Van Caemelbecke E.; Royal. G. In *The Porphyrin Handbook*; Kadish, K. M., Smith, K. M., Guilard, R., Eds.; Academic Press: New York, 2000; Vol. *8*, Chapter *55*, pp 1−114.
(22) Kadish, K. M. *Prog. Inorg. Chem.* **1986**, *34*, 435–605.
(23) Kadish, K. M.; Li, J.; Van Caemelbecke, E.; Ou, Z.; Guo, N.; Autret, M.; D'Souza, F.; Tagliatesta, P. *Inorg. Chem.* **1997**, *36*, 6292–6298.
(24) Anson, F. C.; Shi, C.; Steiger, B. *Acc. Chem. Res.* **1997**, *30*, 437–444.
(25) Doyle, M. P. *Angew. Chem., Int. Ed.* **2009**, *48*, 850–852.
(26) Elbaz, L.; Korin, E.; Soifer, L.; Bettelheim, A. *J. Electroanal. Chem.* **2008**, *621*, 91–96.
(27) Zhang, W.; Shaikh, A. U.; Tsui, E. Y.; Swager, T. M. *Chem. Mater.* **2009**, *21*, 3234–3241.
(28) Skrzypek, D.; Madejska, I.; Habdas, J. *Solid State Sci.* **2007**, *9*, 295–302.
(29) Skrzypek, D.; Madejska, I.; Habdas, J.; Dudkowiak, A. *J. Mol. Struct.* **2008**, *876*, 177–185.
(30) Ziegelbauer, J. M.; Olson, T. S.; Pylypenko, S.; Alamgir, F.; Jaye, C.; Atanassov, P.; Mukerjee, S. *J. Phys. Chem. C* **2008**, *112*, 8839–8849.
(31) Kadish, K. M.; Ou, Z.; Tan, X.; Boschi, T.; Monti, D.; Fares, V.; Tagliatesta, P. *J. Chem. Soc., Dalton Trans.: Inorg. Chem.* **1999**, 1595–1602.
(32) Kadish, K. M.; Guo, N.; Van Caemelbecke, E.; Paolesse, R.; Monti, D.; Tagliatesta, P. *J. Porphyrins Phthalocyanines* **1998**, *2*, 439–450.
(33) Richter-Addo, G. B.; Hodge, S. J.; Yi, G.-B.; Khan, M. A.; Ma, T.; Van Caemelbecke, E.; Guo, N.; Kadish, K. M. *Inorg. Chem.* **1996**, *35*, 6530–6538.
(34) Autret, M.; Ou, Z.; Antonini, A.; Boschi, T.; Tagliatesta, P.; Kadish, K. M. *J. Chem. Soc., Dalton Trans.: Inorg. Chem.* **1996**, 2793–2797.
(35) D'Souza, F.; Villard, A.; Van Caemelbecke, E.; Franzen, M.; Boschi, T.; Tagliatesta, P.; Kadish, K. M. *Inorg. Chem.* **1993**, *32*, 4042–4048.
(36) Mu, X. H.; Kadish, K. M. *Inorg. Chem.* **1990**, *29*, 1031–1036.
(37) Mu, X. H.; Kadish, K. M. *Inorg. Chem.* **1989**, *28*, 3743–3747.
(38) Kadish, K. M.; Lin, X. Q.; Han, B. C. *Inorg. Chem.* **1987**, *26*, 4161–4167.
(39) Wolberg, A.; Manassen, J. *J. Am. Chem. Soc.* **1970**, *92*, 2982–2991.
(40) Walker, F. A.; Beroiz, D.; Kadish, K. M. *J. Am. Chem. Soc.* **1976**, *98*, 3484–3489.

Chart 1. Structures of Investigated Cobalt Porphyrins Where R = 3,5-Di-*tert*-butylphenyl

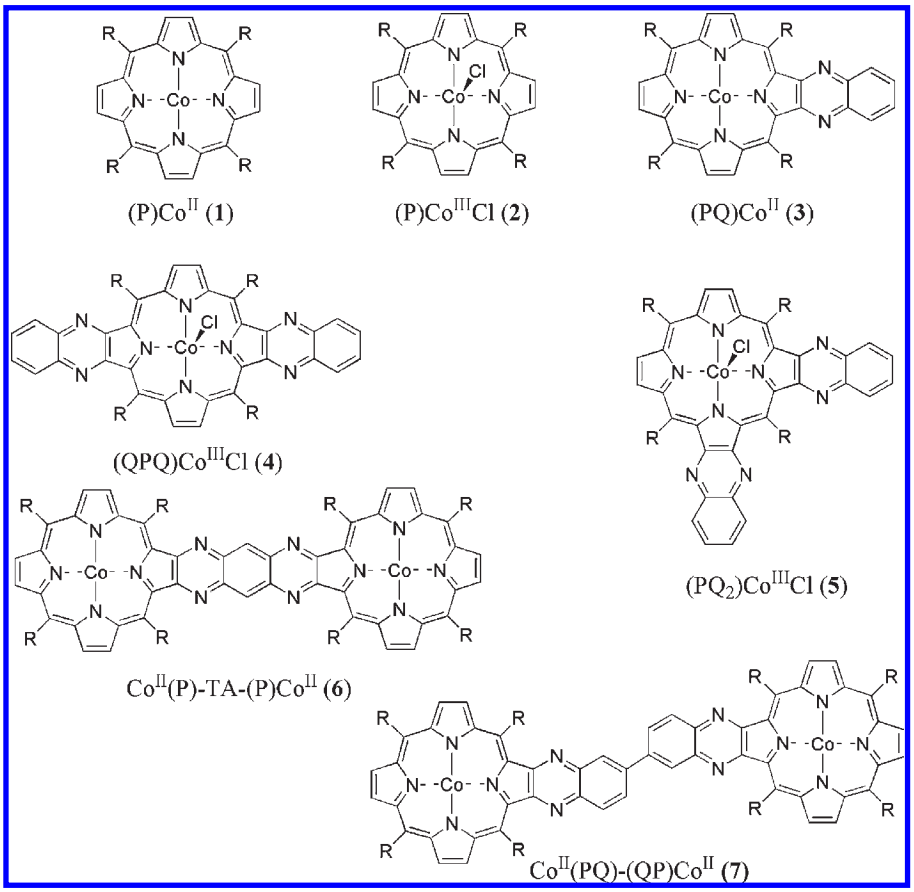

South Wales. Ultraviolet−visible spectra were routinely recorded on a Hitachi 150−20 spectrophotometer in chloroform that was deacidified by filtration through an alumina column. ^{1}H NMR spectra were recorded on a Bruker DPX-400 (400 MHz) spectrometer as stated. Deuteriochloroform was used as the solvent with tetramethylsilane (TMS) as an internal standard. Signals are recorded in terms of chemical shift (in ppm), multiplicity, coupling constants (in Hz), and assignment, in that order. The following abbreviations for multiplicity are used: s, singlet; d, doublet; dd, doublet of doublets; t, triplet; tt, triplet of triplets; m, multiplet; br, broad; ABq, AB quartet. Electrospray ionization (ESI) mass spectra were recorded on a ThermoQuest Finnigan LCQ DECA instrument. Mass spectra were obtained as an envelope of the isotope peaks of the molecular ion. The mass corresponding to the envelope's maxima is reported and was compared with the maxima of a simulated spectrum. High resolution electrospray ionization Fourier transform ion cyclotron resonance spectrometry (HR-ESI-FT/ICR) were recorded on a Bruker Daltonics BioAPEX II FT/ICR mass spectrometer equipped with a 4.7 T MAGNEX superconducting magnet and an Analytical external ESI source. Column chromatography was routinely carried out using the gravity feed column technique on Merck silica gel Type 9385 (230−400 mesh). Analytical thin layer chromatography (TLC) analyses were performed on Merck silica gel 60 F_{254} precoated sheets (0.2 mm). Alumina refers to Merck aluminum oxide 90 active neutral I, type 1077.

Cyclic voltammetry was carried out at 298 K using an EG&G Princeton Applied Research (PAR) 173 potentiostat/galvanostat. A homemade three-electrode cell was used for cyclic voltammetric measurements and consisted of a platinum button or glassy carbon working electrode, a platinum counter electrode, and a homemade saturated calomel reference electrode (SCE). The SCE was separated from the bulk of the solution by a fritted glass bridge of low porosity which contained the solvent/supporting electrolyte mixture.

Thin-layer UV−visible spectroelectrochemical experiments were performed with a home-built thin-layer cell which has a light transparent platinum net working electrode. Potentials were applied and monitored with an EG&G PAR Model 173 potentiostat. Time-resolved UV−visible spectra were recorded with a Hewlett-Packard Model 8453 diode array spectrophotometer. High purity N_2 from Trigas was used to deoxygenate the solution and kept over the solution during each electrochemical and spectroelectrochemical experiment.

Chemicals. All solvents used were routinely distilled prior to use, unless otherwise stated. Light petroleum refers to the fraction of bp 60−80 °C. Ether refers to diethyl ether and was distilled over crushed calcium chloride and stored over sodium wire. Ethanol-free chloroform was obtained by distillation from calcium chloride and passage through alumina. Merck AR grade methanol was used. Where solvent mixtures were used, the proportions are given by volume.

Benzonitrile (PhCN) was obtained from Aldrich Co. and distilled over P_2O_5 under vacuum prior to use. Dichloromethane (CH_2Cl_2) was obtained from Aldrich Co. and used as received for electrochemistry and spectroelectrochemistry experiments. Tetra-*n*-butylammonium perchlorate (TBAP) was purchased from Sigma Chemical or Fluka Chemika Co., recrystallized from ethyl alcohol, and dried under vacuum at 40 °C for at least 1 week prior to use.

{5,10,15,20-Tetrakis(3,5-di-*tert*-butylphenyl)porphyrinato}-cobalt(II) 1. 5,10,15,20- Tetrakis(3,5-di-*tert*-butylphenyl)porphyrin (400 mg, 0.376 mmol) was dissolved in chloroform (20 mL), and a solution of cobalt(II) acetate tetrahydrate (234 mg, 0.940 mmol) in methanol (10 mL) was added. The mixture was heated to reflux with stirring, and TLC indicated immediate completion of the reaction. The solvents were removed, and the

residue purified by chromatography over silica (dichloromethane-light petroleum 1:4). The front running red band was collected, evaporated to dryness, and the resultant residue was recrystallized from dichloromethane-acetonitrile (1:1) to yield {5,10,15,20-tetrakis(3,5-di-*tert*-butylphenyl)- porphyrinato}cobalt(II) **1** (365 mg, 87%) as a dark red-purple microcrystalline solid, mp > 300 °C. MS (ESI): 1120.5 (M^+ requires 1120.5). IR ($CHCl_3$): 3063 w, 3022 m, 2964 s, 2905 m, 2868 m, 1593 s, 1477 m, 1464 m, 1427 m, 1394 m, 1364 s, 1352 m, 1296 m, 1248 m, 1221 s, 1207 s, 1076 w, 1005 m, 930 m cm^{-1}. UV−vis ($CHCl_3$): 413 (log ε 5.46), 530 (4.24) nm. MS (HR-ESI-FT/ICR): m/z 1119.6638, calcd for $[C_{72}H_{92}N_4Co]^+$: 1119.6649.

Chloro{5,10,15,20-tetrakis(3,5-di-*tert*-butylphenyl)porphyrinato}-cobalt(III) 2. {5,10,15,20-Tetrakis(3,5-di-*tert*-butylphenyl)-porphyrinato}cobalt(II) **1** (200 mg, 0.179 mmol) was dissolved in chloroform (100 mL), and methanol (100 mL) and hydrochloric acid (32% w/v, 3 mL) was added. The mixture was stirred for 1 h at which point chloroform (100 mL) was added and the mixture washed with deionized water (3 × 100 mL), dried over anhydrous sodium sulfate, filtered, and the solvent removed. The residue was recrystallized from dichloromethane-acetonitrile (1:1) to yield chloro{5,10,15,20-tetrakis(3,5-di-*tert*-butylphenyl)- porphyrinato}cobalt(III) **2** (194 mg, 94%) as lustrous purple crystals, mp > 300 °C. MS (ESI): 1120.7 ($[M\text{-}Cl]^+$ requires 1120.5). IR ($CHCl_3$): 3062 w, 3022 s, 2966 s, 2905 m, 2870 m, 1593 m, 1477 m, 1466 m, 1427 w, 1394 w, 1364 m, 1352 m, 1296 m, 1248 m, 1225 m, 1213 m, 1200 w, 1080 w, 1005 m, 935 w, 928 w cm^{-1}. UV−vis ($CHCl_3$): 412 (log ε 4.99), 544 (4.03) nm. ^{1}H NMR (400 MHz, $CDCl_3$) δ 1.50 (72 H, br s, *t*-butyl H), 7.80 (4 H, app t, J = 1.8 Hz, *p*-Ar H), 8.04 (4 H, br s, *o*-Ar H), 8.15 (4 H, br s, *o*-Ar H), 8.66 (8 H, s, β-pyrrolic H). ^{1}H NMR (400 MHz, $CDCl_3$-1% d_5-pyridine) δ 1.42 (72 H, s, *t*-butyl H), 7.55 (8 H, d, J = 1.8 Hz, *o*-Ar H), 7.74 (4 H, app t, J = 1.8 Hz, *p*-Ar H), 9.11 (8 H, s, β-pyrrolic H). MS (HR-ESI-FT/ICR): m/z 1119.6653 [M − Cl]$^+$, calcd for $[C_{72}H_{92}N_4Co]^+$: 1119.6649.

{5,10,15,20-Tetrakis(3,5-di-*tert*-butylphenyl)quinoxalino[2,3-*b*′]porphyrinato}cobalt(II) 3. A mixture of 5,10,15,20-tetrakis-(3,5-di-*tert*-butylphenyl)quinoxalino[2,3-*b*′]porphyrin (0.020 g, 0.017 mmol) and cobalt(II) acetate tetrahydrate (0.037 g, 0.147 mmol) in chloroform−methanol (2:1) (21 mL) was heated at reflux under nitrogen for 24 h. The solution was allowed to cool, then filtered through a plug of alumina, washed with dichloromethane, and the solvent removed. Dichloromethane (50 mL) was added to the residue, and the solution washed with deionized water (3 × 50 mL). The organic layers were dried over anhydrous sodium sulfate, and the solvent removed to give a brown-red solid (0.025 g). Recrystallization from dichloromethane-acetonitrile gave {5,10,15,20-tetrakis(3,5-di-*tert*-butylphenyl)quinoxalino-[2,3-*b*′]porphyrinato}cobalt(II) **3** (20 mg, 94%) as a dark red-brown solid, mp. > 300 °C. MS (ESI): 1221.85 (M^+ required 1221.69). IR ($CHCl_3$): 3001 m, 1607 w, 1246 w, 1240 m, 1236 s, 1194 s, 1184 w cm^{-1}. UV−vis ($CHCl_3$): 403 (log ε 5.13), 435 (5.00), 555 (4.52), 598 (4.24) 598 nm. MS (HR-ESI-FT/ICR): m/z 1221.68640 [M − Cl]$^+$, calcd for $[C_{82}H_{94}N_6Co]^+$: 1221.68665.

Chloro{5,10,15,20-tetrakis(3,5-di-*tert*-butylphenyl)bisquinoxalino[2,3-*b*′:12,13-*b*″]pophyrinato}cobalt(III) 4. A mixture of 5,10,15,20-tetrakis(3,5-di-*tert*-butylphenyl)-bisquinoxalino[2,3-*b*′:12,13-*b*″]porphyrin (0.019 g, 0.015 mmol), cobalt(II) acetate tetrahydrate (0.078 g, 0.314 mmol) and anhydrous sodium acetate (0.030 g, 0.362 mmol) in toluene (10 mL) and glacial acetic acid (10 mL) was heated at reflux under nitrogen for 18 h. The solution was allowed to cool, then dichloromethane (50 mL) added and the organic layer washed with deionized water (4 × 50 mL), saturated sodium hydrogen carbonate solution (3 × 50 mL), and deionized water (4 × 50 mL) again. The organic layer was dried over anhydrous sodium sulfate, and the solvent removed. The residue was dissolved in chloroform (10 mL), and concentrated hydrochloric acid (10 M, 1 mL) was added dropwise. The reaction mixture was then stirred at room temperature for 1.5 h. Dichloromethane (30 mL) was added, and the organic layer washed with water (4 × 50 mL). The organic layer was dried over anhydrous sodium sulfate, and the solvent removed to afford chloro{5,10,15,20-tetrakis(3,5-di-*tert*-butylphenyl)bisquinoxalino[2,3-*b*′:12,13-*b*″]porphyrinato} cobalt(III) **4** (0.016 g, 67%) as a dark green solid, mp. > 300 °C. MS (ESI): 1324.73 ($[M - Cl]^+$ required 1358.68). IR ($CHCl_3$): 3043 w, 2989 w, 1551 w, 1240 s, 1194 s cm^{-1}. UV−vis ($CHCl_3$): 356 (log ε 4.57), 417 (4.45), 486 (4.86), 566 (3.70), 615 (3.70), 668 (4.08) nm. MS (HR-ESI-FT/ICR): m/z 1323.70719 [M − Cl]$^+$, calcd for $[C_{88}H_{96}N_8Co]^+$: 1323.70845.

Chloro{5,10,15,20-tetrakis(3,5-di-*tert*-butylphenyl)bisquinoxalino[2,3-*b*′:7,8-*b*″]por-phyrinato}cobalt(III) 5. A mixture of 5,10,15,20-tetrakis(3,5-di-*tert*-butylphenyl)bisquino-xalino[2,3-*b*′:7,8-*b*″]porphyrin (0.036 g, 0.028 mmol), cobalt(II) acetate tetrahydrate (0.141 g, 0.566 mmol), and anhydrous sodium acetate (0.049 g, 0.591 mmol) in toluene (10 mL) and glacial acetic acid (10 mL) was heated at reflux under nitrogen for 48 h. The solution was allowed to cool, then dichloromethane (50 mL) added, and the organic layer washed with deionized water (2 × 75 mL), saturated sodium hydrogen carbonate solution (2 × 75 mL), and deionized water (2 × 75 mL) again. The organic layer was dried over anhydrous sodium sulfate, and the solvent removed. The residue was dissolved in chloroform (10 mL), and concentrated hydrochloric acid (10 M, 1 mL) was added dropwise. The reaction mixture was then stirred at room temperature for 1 h. Dichloromethane (30 mL) was added, and the organic layer washed with water (4 × 50 mL). The organic layer was dried over anhydrous sodium sulfate, and the solvent removed to give chloro{5,10,15,20-tetrakis(3,5-di-*tert*-butylphenyl)bisquinoxalino[2,3-*b*′:7,8-*b*″]porphyrinato}cobalt(III) **5** (0.015 g, 74%) as a dark brown-green solid, mp. > 300 °C. MS (ESI): 1324.87 ($[M - Cl]^+$ required 1358.68). IR ($CHCl_3$): 2964 w, 2392 w, 1263 w, 1229 s, 1213 s, 1202 s cm^{-1}. UV−vis ($CHCl_3$): 351 (log ε 4.65), 413 sh (4.46), 440 (4.56), 483sh (4.52), 507 (4.71), 609 (4.12), 643sh (2.81) nm. MS (HR-ESI-FT/ICR): m/z 1323.70691 [M − Cl]$^+$, calcd for $[C_{88}H_{96}N_8Co]^+$: 1323.70845.

{5,10,16,21,26,31,37,42-Octakis(3,5-di-*tert*-butylphenyl)-44*H*,46*H*,48*H*,50*H*-benzo[1″,2″:5,6;4″,5″:5′,6′]dipyrazine[2,3-*b*:2′,3′-*b*′]bisporphyrinato}cobalt(II) 6. A solution of 5,10,16,21,26,31,37,42-octakis(3,5-di-*tert*-butylphenyl)-44*H*,46*H*,48*H*,50*H*-benzo[1″,2″:5,6;4″,5″:5′,6′]dipyrazine[2,3-*b*:2′,3′-*b*′]bisporphyrin (225 mg, 0.0999 mmol) in chloroform (140 mL) and methanol (15 mL) was heated at reflux with cobalt(II) acetate tetrahydrate (350 mg, 1.405 mmol) for 72 h. Dichloromethane (100 mL) was then added, and the organic phase was washed with water (2 × 100 mL), dried over anhydrous sodium sulfate, and filtered. The filtrate was removed under vacuum, and the residue purified by chromatography over silica (dichloromethane-light petroleum, 1:3). The major band was collected, and the solvent evaporated to dryness to give {5,10,16,21,26,31,37,42-Octakis-(3,5-di-*tert*-butylphenyl)-44*H*,46*H*,48*H*,50*H*-benzo[1″,2″:5,6; 4″,5″:5′,6′]dipyrazine[2,3-*b*:2′,3′-*b*′]bisporphyinato}cobalt(II) **6** (118 mg, 50%) as a brown solid, mp > 300 °C. UV−vis ($CHCl_3$): 422 (log ε 5.35), 449 (5.28), 523 (4.84), 587 (4.28), 662 (4.34) nm. Anal. Calcd for $C_{158}H_{182}N_{12}Co_2$: C, 80.17; H, 7.75; N, 7.1. Found: C, 80.14; H, 7.81; N, 6.8%.

6″,6‴-{5,5′,10,10′,15,15′,20,20′-Octakis(3,5-di-*tert*-butylphenyl)quinoxalino[2,3-*b*:2′,3′-*b*′}bisporphyrinato}cobalt(II) 7. A solution of free-base biquinoxalinyl bis-porphyrin (33 mg, 0.0142 mmol) in chloroform (10 mL) and methanol (15 mL) was heated at reflux with cobalt(II) acetate tetrahydrate (32 mg, 0.146 mmol) for 48 h. Chloroform (100 mL) was then added, and the organic phase was washed with water (2 × 100 mL), dried over anhydrous sodium sulfate, and filtered. The filtrate was removed under vacuum, and the residue recrystallized from a dichloromethane-methanol mixture to afford 6″,6‴-{5,5′,10,10′,15,15′,20,20′-Octakis- (3,5-di-*tert*-butylphenyl)-quinoxalino[2,3-*b*:2′, 3′-*b*′}bisporphyrinato}cobalt(II) **7** (32 mg,

Table 1. Half-Wave Potentials (V vs SCE) of Investigated Compounds in PhCN Containing 0.1 M TBAP

		ring oxidation ($E_{1/2}$)		$Co^{III/II}$		reduction		
#cpd	compound	second	first	E_{pa}[a]	E_{pc}[b]	first	second	third
1	(P)Co	1.35	1.13	0.64	−0.04	−0.87		
2	(P)CoCl	1.27	0.90	0.64	−0.26	−0.87		
3	(PQ)Co	1.19[c]	1.19[c]	0.75	−0.01	−0.70	−1.82[d]	
4	(QPQ)CoCl	1.08	0.90	0.64	−0.24	−0.63	−1.61	−1.91[d]
5	(PQ_2)CoCl	1.10	0.85	0.66	−0.36	−0.64	−1.65	−1.88[d]
6	Co(P)-TA-(P)Co	1.30	1.10	0.75	−0.05	−0.59,−0.73	−1.42	−1.91[d]
7	Co(PQ)-(QP)Co	1.18[c]	1.18[c]	0.67	0.10	−0.69	−1.69	−1.84[d]

[a] Oxidation of Co^{II} to Co^{III}. [b] Reduction of Co^{III} to Co^{II}. [c] Overlapping reactions for generation of π-cation radical and dication. [d] Peak potential at a scan rate of 0.10 V/s.

92%) as a brown microcrystalline powder, mp > 300 °C. UV−vis ($CHCl_3$): 413 (log ε 5.34), 453sh (5.17), 520sh (4.44), 562 (4.53), 603 (4.43) nm. MS (HR-ESI-FT/ICR): m/z 1221.685799 (M^{2+}), calcd for $[C_{164}H_{186}N_{12}Co_2]^{2+}$: 1221.68435.

Results and Discussion

Synthesis. Synthesis of the cobalt porphyrins **1**, **3**, **6**, and **7** were carried out using standard metalation procedures, that is, refluxing a solution of the corresponding free-base macrocycle and cobalt(II) acetate tetrahydrate in chloroform and methanol, solvents that solubilize both reagents. IR spectra of the metalated products indicated the absence of inner NH free-base porphyrin stretches, and mass spectral analysis showed the appropriate molecular ion of the cobalt porphyrin. UV−vis spectra were characterized by two major Q bands, also indicating cobalt(II) chelation. In addition, sharp ^{1}H NMR spectra were not obtained, consistent with the paramagnetic character of these compounds.

The cobalt(II) metalation procedure described above failed to work for the free-base bisquinoxalinoporphyrins **4** and **5**, and a solution containing toluene and glacial acetic acid with excess sodium acetate salt was used to facilitate metalation in these cases. During the course of the reaction the color of the mixture turned dark green as Co(III) was generated.[41] This oxidation is feasible as ligands, in particular those bearing oxygen groups (e.g., CO, NO),[21]can facilitate conversion to Co(III) in the presence of oxygen. However, to be certain of obtaining a pure Co(III) porphyrin material after workup, the reaction products were directly converted to their corresponding cobalt(III) chloride form by refluxing the chelate in a solution containing concentrated HCl giving **4** and **5** as the final products. UV−visible spectroscopy of **4** suggests both the metal-centered oxidation and the presence of a chloride axial ligand. The Q-band at 609 nm and the shoulder at 643 nm in **5** are both red-shifted in comparison to other metal(II) complexes. For example, the corner copper(II) bisquinoxalinoporphyrin, (PQ_2)Cu, has Q bands at 561 and 602 nm.[14] The UV−visible spectrum of **5** also has three peaks in the Q-band region located at 668, 615, and 566 nm, and this differs from the spectrum of the oxidized copper(II) analogue where electron abstraction occurs from the conjugated macrocycle.[14]

^{1}H NMR analysis of **5** gave broad spectra as expected for a cobalt(III) porphyrin.[42,43]

(P)Co^{III}Cl **2** was prepared in high yield from its corresponding cobalt(II) analogue by stirring a chloroform solution of **1** in the presence of concentrated hydrochloric acid for 1 h. The Q-band is red-shifted from 529 nm in **1** to 544 nm **2**, confirmed axial chelation. Furthermore, to minimize the presence of a high spin state cobalt(III) which would complicate NMR analyses, 1% d_5-pyridine was added to deuterated chloroform. Under these solution conditions the chloride ligand in **2** was displaced by pyridine, leading to a well-resolved spectrum which could be fully assigned, thus confirming the structural integrity and oxidation state of this compound.

Electrochemistry. The electrochemistry of each compound was carried out in PhCN containing 0.1 M TBAP. The reduction and oxidation potentials are summarized in Table 1 which is divided into three groups: (i) the Co(II) and Co(III) tetrakis(3,5-di-*tert*-butylphenyl)porphyrins **1** and **2**; (ii) the mono and bis-quinoxalinoporphyrin derivatives **3**, **4**, and **5**, and (iii) the linked bis-cobalt quinoxalinoporphyrins **6** and **7**. The redox behavior of these three groups is described below.

Tetrakis(3,5-di-*tert*-butylphenyl)porphyrins 1 and 2. The electrochemistry of synthetic Co(II) and Co(III) porphyrins has been reported under numerous solution conditions.[21−40] Up to five redox reactions can be observed depending upon the positive and negative potential limits of the utilized solvent/supporting electrolyte system. Most Co(II) porphyrins in nonaqueous media undergo one or two reductions which are virtually independent of the solvent and supporting electrolyte, consistent with a relatively weak axial ligand binding to Co(II) and the lack of any solvent or ligand binding to Co(I).[21] Derivatives with highly electron-withdrawing substituents may also undergo three reductions, one at the cobalt center and two at the macrocycle.[44] Three oxidations may also be seen for many synthetic Co(II) porphyrins in nonaqueous media with a large positive potential range such as CH_2Cl_2 or PhCN. The first oxidation occurs at a potential which is highly dependent upon both the solvent/supporting electrolyte mixture and the type of axial ligand on the singly oxidized species.[21] The first electron abstraction from Co(II) porphyrins has in almost all cases been assigned as leading to formation of a Co(III) complex but in rigorously dry CH_2Cl_2 with

(41) Fox, M. A.; Grant, J. V.; Melamed, D.; Torimoto, T.; Liu, C.-Y.; Bard, A. J. *Chem. Mater*. **1998**, *10*, 1771–1776.
(42) Chapman, R. D.; Fleischer, E. B. *J. Chem. Soc., Chem. Commun*. **1981**, 332–333.
(43) Chapman, R. D.; Fleischer, E. B. *J. Am. Chem. Soc*. **1982**, *104*, 1582–1587.
(44) Lin, X. Q.; Boisselier-Cocolios, B.; Kadish, K. M. *Inorg. Chem*. **1986**, *25*, 3242–3248.

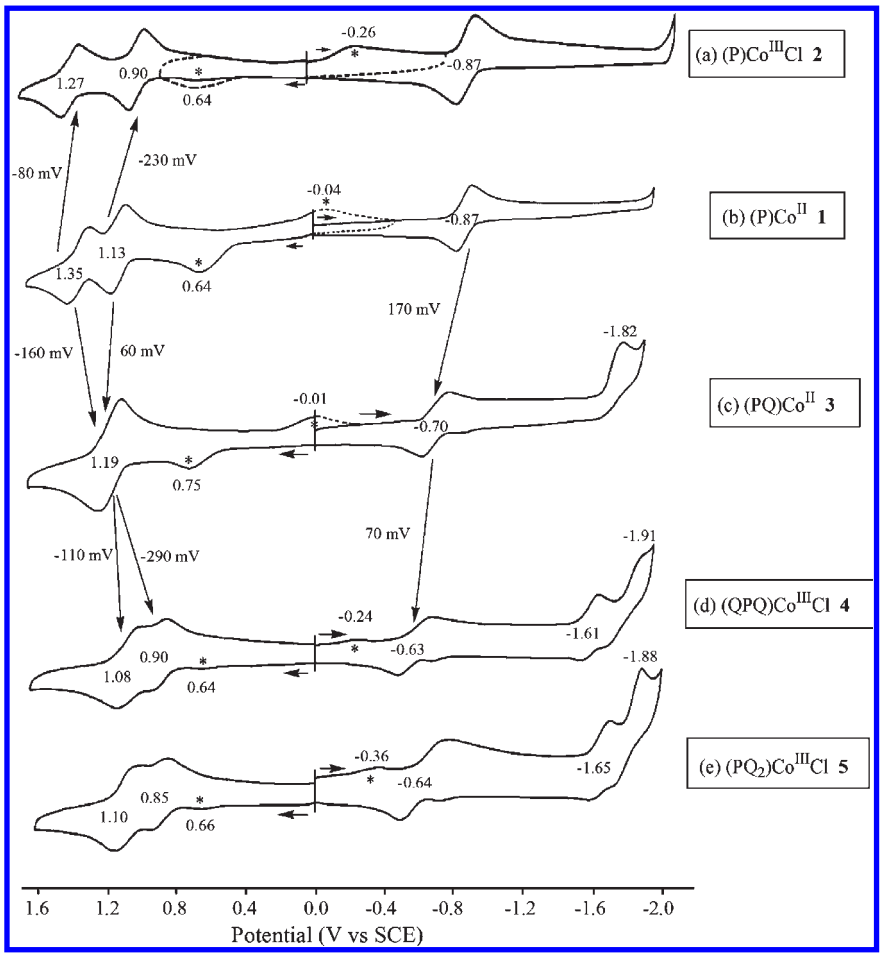

Figure 1. Cyclic voltammograms of (P)Co^{II} **1**, (P)$Co^{III}Cl$ **2**, (PQ)Co^{II} **3**, (QPQ)$Co^{III}Cl$ **4**, and (PQ_2)$Co^{III}Cl$ **5** in PhCN, 0.1 M TBAP.

weakly coordination axial ligands, a Co(II) porphyrin π-cation radical has been shown to exist. Whatever the site of electron transfer in the first one-electron oxidation, two additional one-electron abstractions will occur to give the doubly and triply oxidized porphyrins, the latter of which has been assigned as a Co(III) porphyrin dication.[21]

The electrochemistry of (P)Co^{II} examined in the present study is similar to that of the well-characterized (TPP)Co^{II} under the same solution conditions.[21,22,39] The Co(II)/Co(I) process of (P)Co^{II} occurs at $E_{1/2}$ = −0.87 V in PhCN, but the expected second reduction is located beyond the negative potential limit of the solvent and is not observed at room temperature. Like in the case of (TPP)Co^{II}, the Co(II)/Co(III) reaction of (P)Co^{II} is irreversible, consistent with two non-coupled redox processes. One is an oxidation of (P)Co^{II} followed by ClO_4^- binding to the product (an electrochemical *EC* mechanism) and the other a re-reduction of (P)$Co^{III}ClO_4$ followed by loss of ClO_4^- (also an *EC* mechanism). The anodic peak for oxidation of (P)Co^{II} in PhCN is located at E_{pa} = 0.64 V for a scan rate of 0.1 V/s while the cathodic peak for re-reduction of (P)$Co^{III}ClO_4$ is located at E_{pc} = −0.04 V. Both processes are indicated by an asterisk (*) in Figure 1b. Similar reactions have been reported for numerous other cobalt porphyrins where a classic box mechanism has been proposed,[21,22] and, as described later in this manuscript, it is also observed for all seven compounds investigated in the current study.

As shown in Figure 1b and Scheme 1, the electrogenerated (P)$Co^{III}ClO_4$ undergoes two oxidations at $E_{1/2}$ = 1.13 and 1.35 V, both of which are reversible to stepwise give a Co(III) π-cation radical and dication.

The first one-electron reduction and re-oxidation of (P)$Co^{III}Cl$ **2** in PhCN (Figure 1a) can also be described by a box mechanism with two non-coupled redox reactions, each involving an *EC* mechanism as shown in Scheme 1. The neutral Co(III) porphyrin is characterized by a one-electron reduction at E_{pc} = −0.26 V to give $[(P)Co^{II}Cl]^-$ while the one-electron re-oxidation proceeds via (P)Co^{II} after a rapid loss of Cl^- from the reduction product and is characterized by an anodic peak at E_{pa} = 0.64 V on the reverse sweep for a scan rate of 0.1 V/s (also marked with an asterisk in Figure 1a). Two reversible one-electron oxidations of (P)$Co^{III}Cl$ are located at $E_{1/2}$ = 0.90 and 1.27 V and are shifted to less positive potentials as compared to the same redox processes of electrogenerated (P)$Co^{III}ClO_4$ ($E_{1/2}$ = 1.13 and 1.35 V) in 0.1 M TBAP (Table 1 and Figure 1). This negative shift in $E_{1/2}$ for the two ring-centered oxidations of the chloride bound species amounts to 230 and 80 mV (see Figures 1a,b) and results from an increased anion binding constant for the higher oxidized forms of the porphyrin as compared to its reduced form.

The overall combined mechanism for the oxidation and reduction of (P)$Co^{III}Cl$ and (P)Co^{II} is shown in Scheme 1 where redox processes of the ClO_4^- coordinated porphyrin are illustrated in the top row of the scheme and the

Scheme 1. Proposed Mechanism for Oxidation and Reduction of $(P)Co^{II}$ and $(P)Co^{III}Cl$ in PhCN, 0.1 M TBAP

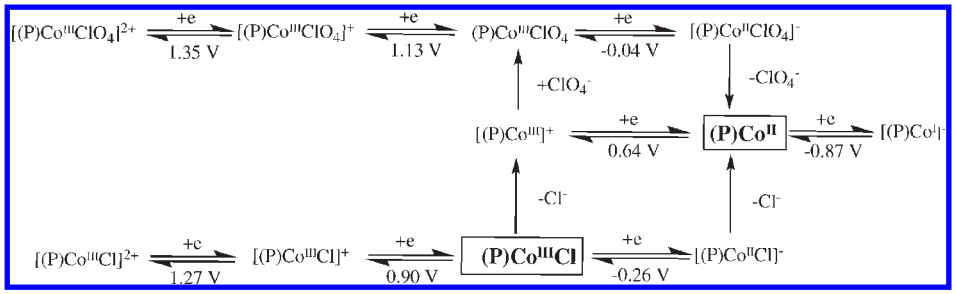

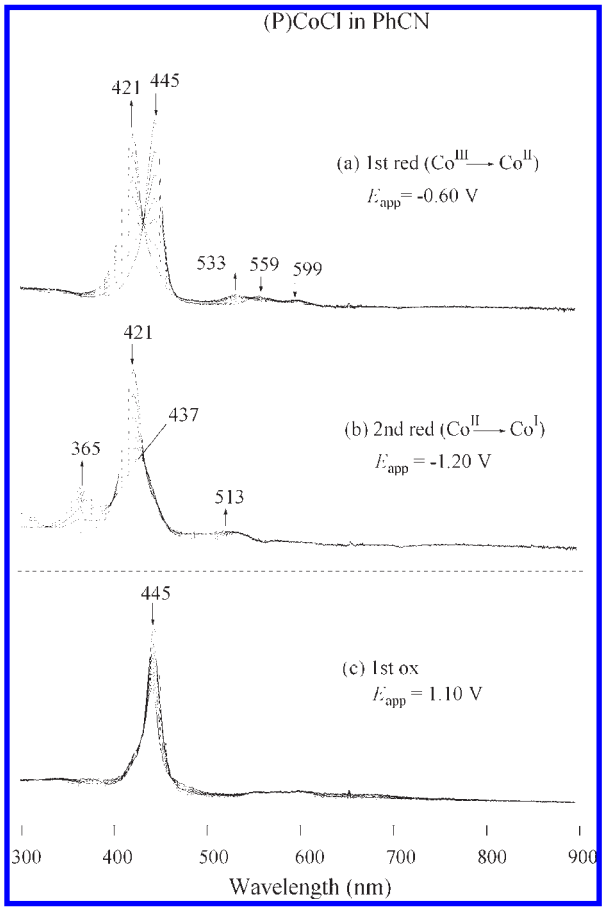

Figure 2. UV−visible spectral changes of $(P)Co^{III}Cl$ **2** during controlled potential (a) reduction at −0.60 V ($Co^{III} \rightarrow Co^{II}$), (b) reduction at −1.20 V ($Co^{II} \rightarrow Co^{I}$), and (c) oxidation at 1.10 V in PhCN containing 0.1 M TBAP.

Cl^- bound porphyrin is at the bottom. It should be noted that the same Co^{II}/Co^{I} redox process is seen for both compounds at −0.87 V in PhCN, and the same UV−visible spectrum is also obtained as a reduction product independent of the oxidation state of the starting compound. This is not surprising since the same $(P)Co^{II}$ species is reduced to an identical product in each case, that is, $[(P)Co^{I}]^-$.

UV−visible spectral changes for the stepwise conversion of $(P)Co^{III}Cl$ to $(P)Co^{II}$ (E_{pc} = −0.26 V) and then to $[(P)Co^{I}]^-$ ($E_{1/2}$ = −0.87 V) in PhCN are shown in Figures 2a,b. This figure also shows the spectral changes for formation of the Co(III) π-cation radical during controlled potential oxidation at 1.10 V (Figure 2c). A summary of the absorption maxima is given in Table 2 which also includes results for (TPP)Co taken from the literature. As seen from the table, the peak maxima for (P)CoCl **2** in its neutral and reduced forms are quite similar to peak maxima for the TPP derivatives in the same oxidation states and solvent.[35] Neither singly reduced $(P)Co^{II}$ nor singly reduced $(TPP)Co^{II}$ has a band in the near-IR region of the spectrum, thus ruling out assignment of a Co(II) π-anion radical as the reduction product.

Mono and Bis-quinoxalinoporphyrins 3−5. The redox behavior of the three monocobalt quinoxalinoporphyrins, $(PQ)Co^{II}$, $(QPQ)Co^{III}Cl$, and $(PQ_2)Co^{III}Cl$, parallels in part what was previously described for quinoxalinoporphyrins with other central metal ions,[3,5,8,14] but significant differences are observed for the currently investigated compounds as described below.

Comparison of $(PQ)Co^{II}$ with $(P)Co^{II}$. Several major differences are seen in the cyclic voltammograms of $(PQ)Co^{II}$ **3** and $(P)Co^{II}$ **1** (Figure 1b,c). The first reduction of $(PQ)Co^{II}$ occurs at −0.70 V as compared to −0.87 V for $(P)Co^{II}$ and this 170 mV positive shift in $E_{1/2}$ is similar to what was previously reported for upon going from $(P)M^{II}$ to $(PQ)M^{II}$ (M = Zn, Cu, Ni, or Pd) where the average $\Delta E_{1/2}$ was also 170 mV.[8] However, the spectroelectrochemical data suggest a different site of electron transfer for the first reduction of the two cobalt porphyrins, being metal-centered in the case of $(P)Co^{II}$ and a mixture of metal and ring-centered in singly reduced $(PQ)Co^{II}$ **3**. A second one-electron reduction of $(PQ)Co^{II}$ can also be seen in PhCN and is assigned to a metal-centered reduction on the basis of the spectroelectrochemical data. This reaction is not seen for $(P)Co^{II}$ in the current study but has been reported to occur at $E_{1/2}$ = −1.97 V for (TPP)Co under similar solution conditions.

Unlike the 170 mV difference in $E_{1/2}$ for the first reduction of $(P)Co^{II}$ and $(PQ)Co^{II}$, much smaller differences in potential are observed in the non-coupled $Co^{II} \rightarrow Co^{III}$ and $Co^{III} \rightarrow Co^{II}$ reactions of the same two compounds (Figure 1). The second and third one-electron oxidations of $(PQ)Co^{II}$ are overlapped in potential, and the peak current for this process at $E_{1/2}$ = 1.19 V is approximately double that for the reduction at −0.70 V under the same experimental conditions. This indicates an electrochemical mechanism involving two overlapping one-electron oxidations (an electrochemical *EE* mechanism) as opposed to a global two-electron abstraction where the diffusion controlled peak current would be proportional to $n^{3/2}$ or 2.77 times larger than a one-electron transition.[45] An overlap of oxidation potentials

(45) Bard, A. J.; Faulkner, L. R. *Electrochemical Methods, Fundamental and Applications*, 2nd ed.; John Wiley & Sons, Inc: New York, 2001.

Table 2. UV-Visible Spectra Data (λ_{max}, nm)[a] Showing Soret and near-IR Bands of the Neutral, Oxidized, and Reduced Cobalt Porphyrins in PhCN

	λ_{max}, nm						
compound	TPP[b]	P	PQ	QPQ	PQ_2	P-TA-P[c]	PQ-QP[c]
$[(Por)Co^{III}]^+$	441, 553, 588	**445, 559, 599**	349, 420, 468	**360, 420, 486**	**353, 440, 508**	446, 472	430, 476
$(Por)Co^{II}$	**417, 531**	421, 533	**414, 445**	411, 447	410, 505	**426, 459**	**423, 472**
$[(Por)Co]^-$	364, 428, 514	365, 437, 513	414, 445, 792	405, 454, 814	410, 441, 750	369, 426, 780	423, 472, 853
$[(Por)Co]^{2-}$			372, 435	380, 407	373, 410,	372, 430, 793	372, 421

[a] Bold data for neutral compound. [b] Data taken from ref 35. [c] Data for reduction or oxidation of two porphyrin units.

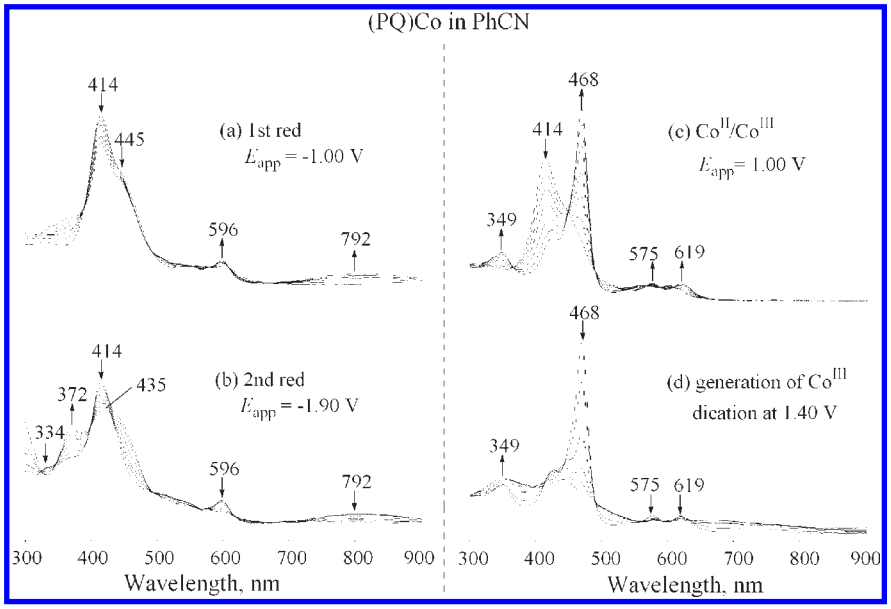

Figure 3. UV−visible spectral changes of $(PQ)Co^{II}$ **3** during controlled potential reduction and oxidation in PhCN, 0.1 M TBAP.

and direct conversion of the neutral porphyrin to its dication form was previously reported for $(PQ)H_2$ and (PQ)Ni in PhCN and is also known to occur in non-coordinating media for a variety of nickel porphyrins with other macrocycles.[46]

An overlapping of two porphyrin oxidations has been observed in low dielectric constant media such as toluene, heptane, or benzene[47,48] and results from a stronger binding of the doubly oxidized porphyrin with an anion from the supporting electrolyte or the original counterion in the case of porphyrin with M(III) central metal ions. In the case of electrogenerated $[(PQ)Co^{III}]^{2+}$, the shift in potential for the second oxidation amounts to 160 mV when compared to compound **1**.

UV−visible spectra were also monitored in a thin-layer cell during each electron transfer process of $(PQ)Co^{II}$ in PhCN, and the resulting data are shown in Figure 3 and Table 2. The two reductions of $(PQ)Co^{II}$ are presented in parts *a* and *b* of the figure, and the two oxidations in parts *c* and *d*. Several isosbestic points are obtained, indicating the absence of spectrally detectable intermediates. The two reductions of $(PQ)Co^{II}$ each involve a one-electron addition to give $[(PQ)Co]^-$ and $[(PQ)Co]^{2-}$ while the two oxidations are characterized by an initial one-electron abstraction to give $[(PQ)Co^{III}]^+$ (λ_{max} = 349, 420, and 468 nm) followed by a global two-electron abstraction to give the Co(III) porphyrin with a doubly oxidized macrocycle (an electrochemical *EE* mechanism as described above).

A different site of electron transfer is proposed for the first one-electron reduction of $(PQ)Co^{II}$ **3** compared to that of $(P)Co^{II}$ **1**. The singly reduced product of $(P)Co^{II}$ is assigned as $[(P)Co^{I}]^-$ and has a split Soret band at 365 and 437 nm (see Table 2). This contrasts with the UV−visible spectrum of electrogenerated $[(PQ)Co^{II}]^-$ which has a split Soret band at 414 and 445 nm, as well as a broadband in the near-IR region of the spectrum centered at 792 nm (Figure 3a). This latter near-IR band is diagnostic of a porphyrin π-anion radical,[21] suggesting that the first electron added to $(PQ)Co^{II}$ resides in part on the porphyrin π-ring system where the $[(PQ)Co]^-$ product is assigned as a Co(II) π-anion radical with Co(I) porphyrin character.

The controlled potential of reduction of $(PQ)Co^{II}$ at −1.90 V then leads to $(PQ)Co^{I}]^{2-}$, and the resulting spectral changes during this process are illustrated in Figure 3b. The final spectrum at the completion of electrolysis is characterized by a split Soret band at 372 and 435 nm. Similar absorption bands at 365 and 437 nm are seen in the UV−visible spectrum of $[(P)Co^{I}]^-$ (Table 2 and Figure 2b) suggesting the possibility of protonation on the quinoxaline nitrogen to give $[(PQH)Co^{I}]^-$ as described in the literature for (PQ)Ni, (PQ)Cu, and

(46) Kadish, K. M.; Lin, M.; Van Caemelbecke, E.; Stefano, Q. D.; Medforth, C. J.; Nurco, D. J.; Nelson, N. Y.; Krattinger, B.; Muzzi, C. M.; Jaquinod, L.; Xu, Y.; Shyr, D. C.; Smith, K. M.; Shelnutt, J. A. *Inorg. Chem.* **2002**, *41*, 6673–6687.
(47) Mu, X. H.; Lin, X. Q.; Kadish, K. M. *Electroanlysis* **1989**, 113–116.
(48) Geng, L.; Ewing, A. G.; Jernigan, J. C.; Murray, R. W. *Anal. Chem.* **1986**, *58*, 852–860.

$(PQ)SnX_2$ (X = OH^- or Cl^-) after reaction of the electrogenerated dianion with trace water in CH_2Cl_2.[5] This type of reaction was not confirmed or characterized in the case of doubly reduced $(PQ)Co^{II}$ because of the extremely negative reduction potential needed for generation of the anionic species in PhCN (−1.90 V).

(QPQ)Co^{III}Cl 4 and (PQ$_2$)Co^{III}Cl 5. Cyclic voltammograms of **4** and **5** are shown in Figure 1 which also includes voltammetric data for **1**−**3**. As seen in the figure, reduction peak potentials for the non-coupled Co^{III}/Co^{II} process of $(P)Co^{III}Cl$ **2** and $(QPQ)Co^{III}Cl$ **4** are virtually identical to each other and shifted negatively from the reduction peak potentials of **1** and **3** where the product of the one-electron oxidation is a Co(III) porphyrin containing ClO_4^- from the TBAP supporting electrolyte.

In general, the larger the formation constant between $[(Por)Co^{III}]^+$ and an anionic axial ligand (Cl^- or ClO_4^-), the more negative will be the reduction potential,[49] and this is what is observed in the present case. For example, the E_{pc} = −0.24 V for the Co^{III}/Co^{II} reaction of **4** indicates a stronger Cl^- binding to $[(QPQ)Co]^+$ as compared to $[(P)Co^{III}]^+$ which is reduced at E_{pc} = −0.04 V. $(PQ_2)CoCl$ **5** is reduced at E_{pc} = −0.36 V (Figure 1e), which indicates an even stronger Cl^- binding in the case of $[(PQ_2)Co]^+$.

In contrast to the Co(III) reduction potentials which depend on the counterion, the peak potentials for oxidation of the Co(II) porphyrins to their $Co^{III}-ClO_4^-$ form are almost the same for all of the investigated compounds, being equal to 0.64 to 0.66 V in **1**, **2**, **4**, and **5** and 0.75 V in **3**. An identical $E_{1/2}$ is also obtained for the first ring-centered oxidation of **2** and **4** (0.90 V), indicating that the presence or absence of the two linear fused Q groups on the macrocycle has no effect on the oxidation processes. However, differences in potential do exist in the second reduction of the same two Co(III) porphyrins which is located at $E_{1/2}$ = −0.87 V in **2** and −0.63 V in **4**. Two additional reductions of **4** are also seen at $E_{1/2}$ = −1.61 and E_{pc} = −1.91 V, neither of which can be measured for $(P)Co^{II}$ **1** or $(P)Co^{III}Cl$ **2** in the PhCN solvent whose cut off is approximately −1.90 V.

Thin-layer UV−visible spectral changes during the first three reductions of $(QPQ)Co^{III}Cl$ **4** are shown in Figure 4, and peak maxima for the neutral and electroreduced form of the porphyrin are summarized in Table 2. Initially, the potential was set at 0.70 V to oxidize any trace $(QPQ)Co^{II}$ in solution, thus giving a pure spectrum of $(QPQ)Co^{III}Cl$ which is characterized by three bands at 360, 420, 486 nm in the Soret region. There is also a visible band at 669 nm. The product of the first reduction at an applied potential of −0.50 V exhibits a split Soret band at 411, 447 nm and a visible band at 652 nm (Figure 4a). This spectrum is characteristic of a (PQ)M species (M = Cu^{II}, Zn^{II}, Ni^{II}, Pd^{II} or Au^{II}),[4,7,8] thus confirming that the Co^{II} form of compound **5** is electrogenerated under the given solution conditions.

The final reduction product after the second controlled potential electrolysis of (QPQ)CoCl at −0.90 V exhibits a split Soret band at 405 and 454 nm, as well as a diagnostic π-radical band at 814 nm (Figure 4b and Table 2). This species is assigned as having both Co(I) porphyrin and

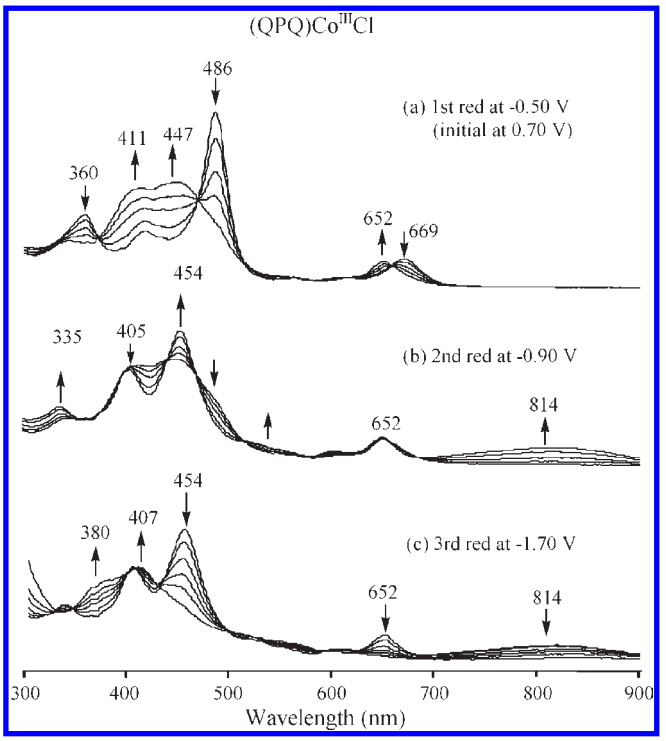

Figure 4. UV−visible spectral changes of $(QPQ)Co^{III}Cl$ **4** during reductions at (a) −0.50 V, (b) −0.90 V, (c) −1.70 V in PhCN, 0.1 M TBAP (the initial spectrum is obtained at 0.70 V).

Co^{II} π-anion radical character. The third electroreduction of (QPQ)CoCl **4** at −1.70 V leads to a pure Co(I) porphyrin based on the spectral changes illustrated in Figure 4c. Finally, the spectral changes obtained during the oxidation of (QPQ)CoCl at 1.00 and 1.20 V indicate formation of a Co^{III} porphyrin π-cation radical and dication, respectively, in PhCN, 0.1 M TBAP (Supporting Information, Figure S1).

Similar electrochemistry and spectroelectrochemistry is observed for $(PQ_2)Co^{III}Cl$ **5** which undergoes four reductions and two oxidations in PhCN (Figure 1e). The potentials for all six redox processes of **5** are close to those of $(QPQ)Co^{III}Cl$ **4**, a result not observed for previously examined QPQ and PQ_2 derivatives with other metal ions where the differences in $E_{1/2}$ are large.[14] The spectral changes observed during reduction and oxidation of (PQ_2)-CoCl **5** are also similar to those of (QPQ)CoCl **4** under the same experimental conditions and are shown in Supporting Information, Figure S2. Because of these similarities, the same reduction/oxidation mechanism is proposed for this compound as for **4** which is described above.

TA Linked Bis-cobalt Dyad 6. Co(P)-TA-(P)Co **6** undergoes three oxidations and four reductions in PhCN as illustrated in Figure 5. The first oxidation involves a non-coupled Co^{II}/Co^{III} transition like described earlier for the other compounds, and this is followed by two reversible ring-centered reactions at $E_{1/2}$ = 1.10 and 1.30 V versus SCE. The shape of the current−voltage curve for oxidation of **6** and the potentials of each process are close to those of (P)Co **1**, as would be expected for two non-interacting $(P)Co^{II}$ macrocycles linked to each other by a fused TA group. The main difference in electrochemical behavior between **6** and **1** is that each redox process involves a global two-electron abstraction in the dyad

(49) Truxlllo, L. A.; Davis, D. G. *Inorg. Chem.* **1975**, *47*, 2260–2267.

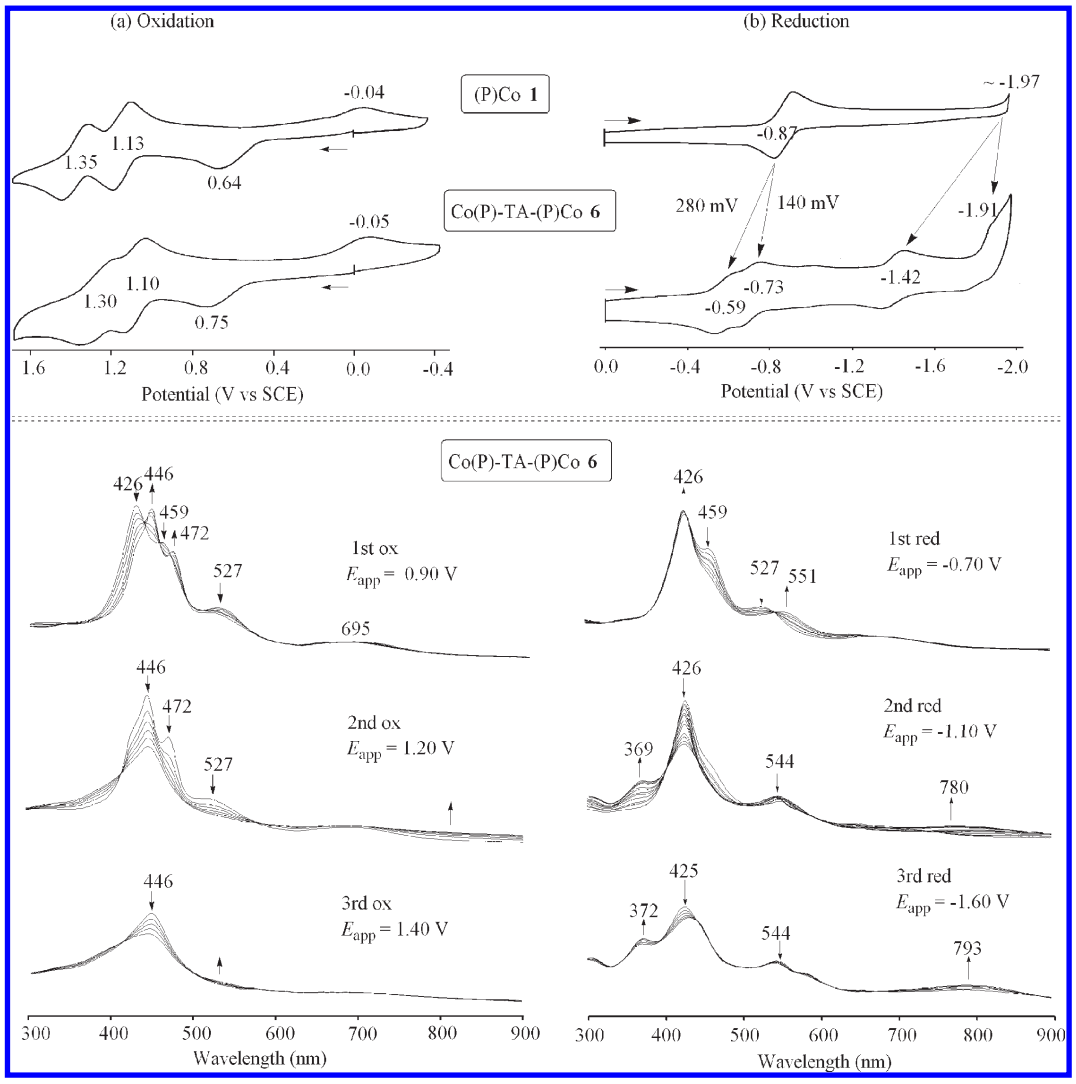

Figure 5. Cyclic voltammograms and UV−visible spectral changes for (a) oxidation and (b) reduction Co^{II}(P)-TA-(P)Co^{II} **6** in PhCN, 0.1 M TBAP.

with no difference in the potentials as compared to the monocobalt macrocycle, indicating equivalent non-interacting redox centers.

The anodic peak potential for conversion of Co(II) to Co(III) is shifted from 0.64 V in **1** to 0.75 V in **6** while the reverse Co(III)/Co(II) process appears at $E_{pc} = -0.05$ V. The mechanism for the Co^{II}/Co^{III} process is the same as shown in Scheme 1 with the only difference being the peak potential for oxidation which is 0.75 V in **6** and (PQ)Co^{II} **3**, but 0.64 to 0.66 V for all of the other compounds (see Figure 1c and Table 1). It should also be noted that the two porphyrin ring-centered oxidations of **6** (eqs 1 and 2) are shifted negatively by 30−50 mV with respect to $E_{1/2}$ for the same two reactions of the monocobalt compound **1**, consistent with a small electron-donating effect of the fused TA unit which would lead to easier oxidations.

$$[Co^{III}(P)\text{-}TA(P)Co^{III}]^{2+} \leftrightharpoons [Co^{III}(P)\text{-}TA(P)Co^{III}]^{4+} + 2e \quad (1)$$

$$[Co^{III}(P)\text{-}TA(P)Co^{III}]^{4+} \leftrightharpoons [Co^{III}(P)\text{-}TA(P)Co^{III}]^{6+} + 2e \quad (2)$$

The UV−visible spectra obtained after each oxidation of **6** in a thin-layer cell are shown in Figure 5a, with the final oxidation products exhibiting bands found in both electrooxidized (P)Co^{II} **1** and (PQ)Co^{II} **3**. For example, the global $2e^-$ oxidation of **6** (eq 1) at 0.90 V leads to a Co(III) spectrum with bands at 446 and 472 nm one of which is comparable to a 445 nm band in the spectrum of $[(P)Co^{III}]^+$ (Table 1 and Figure 1) and the other to a 468 nm band in the spectrum of $[(PQ)Co^{III}]^+$ (Table 1 and Figure 3c).

A following second $2e^-$ oxidation of **6** at 1.12 V occurs at the porphyrin macrocycle and leads to a spectrum with a band at 446 nm. A similar band appears at 445 nm in the spectrum of (P)CoCl **2** after the first ring-centered oxidation. Finally, the third global two-electron oxidation of **6** (eq 2) at 1.40 V leads to an almost total loss of intensity in all bands, and this is seen for most porphyrin dications.

The electrochemical and spectroscopic data for the oxidation of **6** are thus self-consistent in showing a lack of interaction between the two porphyrin units of the dyad across the TA bridge, but this is not the case for reduction as seen in Figure 5a, where four one-electron reductions are observed as compared to

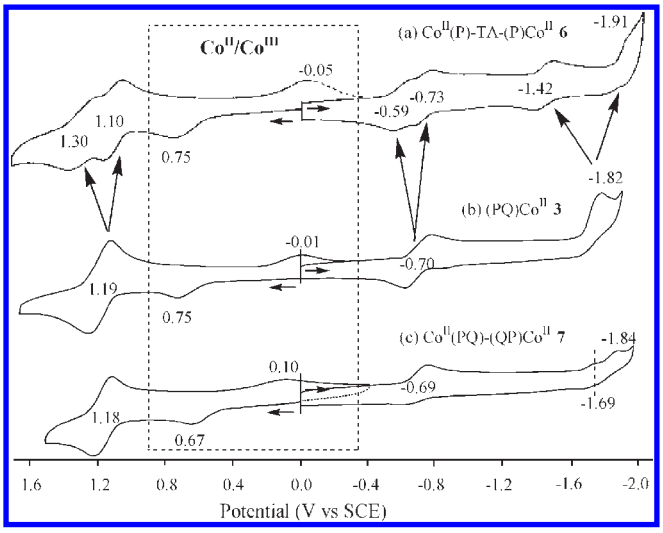

Figure 6. Cyclic voltammograms of (a) Co^{II}(P)-TA-(P)Co^{II} **6**, (b) (PQ)Co^{II} **3**, and (c) Co^{II}(PQ)-(QP)Co^{II} **7** in PhCN, 0.1 M TBAP.

just one reduction in the case of (P)Co **1**. The four reductions of **6** are proposed to occur as shown in eqs 3−6 and give four different Co(P)-TA-(P)Co reduction products, two of which are assigned as "half reduced" dyads.

$$\text{Co(P)-TA-(P)Co} + e \leftrightarrows [\text{Co(P)-TA(P)Co}]^- \quad (3)$$

$$[\text{Co(P)-TA-(P)Co}]^- + e \leftrightarrows [\text{Co(P)-TA(P)Co}]^{2-} \quad (4)$$

$$[\text{Co(P)-TA-(P)Co}]^{2-} + e \leftrightarrows [\text{Co(P)-TA(P)Co}]^{3-} \quad (5)$$

$$[\text{Co(P)-TA-(P)Co}]^{3-} + e \leftrightarrows [\text{Co(P)-TA(P)Co}]^{4-} \quad (6)$$

The difference in potentials between the first reduction of **6** at $E_{1/2} = -0.59$ V and the second at $E_{1/2} = -0.73$ V (eqs 3 and 4) amounts to 140 mV while the third and fourth reductions (eqs 5 and 6) differ by almost 500 mV. These separations can be compared to the $\Delta E_{1/2}$ values which range from 150 to 300 mV for interacting redox centers of bis-porphyrin[50] and bis-corrole[51,52] dyads linked in a face-to-face arrangement, thus indicating a stronger interaction between the singly and the doubly reduced porphyrin units of **6** than for the dyad in its neutral Co^{II} form.

Although the electrochemistry of the dyad **6** can be analyzed in terms of two (P)Co^{II} macrocycles linked by a fused TA bridge, comparisons should also be made between the redox reactivity of **6** and that of **3** which has a single fused quinoxaline group. This comparison is shown in Figure 6 which also includes a cyclic voltammogram of the single bond connected dyad **7** discussed in the following section. It is interesting to note that peak potentials for the $Co^{II} \rightarrow Co^{III}$ and $Co^{III} \rightarrow Co^{II}$ processes of **6** and **3** are virtually identical in the two compounds, but this is not the case for the other redox reactions of these same two compounds as seen in Figures 5 and 6.

The similarity in oxidation potential for the $Co^{II} \rightarrow Co^{III}$ reactions of (PQ)Co^{II} **3** and Co^{II}(P)-TA(P)Co^{II} **6** is also reflected in the similar UV−visible spectra of the two compounds (see Table 2). The spectrum of neutral **6** is similar to that of the (PQ)Co^{II} **3** derivative in that it has a split Soret band (426 and 459 nm) like most other (PQ)M^{II} porphyrins.[8] The 426 nm band of **6** is also comparable to a band at 421 nm in the spectrum of (P)Co^{II} (see Table 2). Generation of the half reduced species at a controlled potential reduction at −0.70 V (eq 3) then leads to a loss of the 459 nm band, a slight increase in intensity of the band at 426 nm and the appearance of a new Q-band at 551 nm. There are also well-defined isosbetic points as seen in Figure 5b. The spectrum of this singly reduced product closely resembles the UV−visible spectrum of neutral (P)Co^{II} (λ_{max} = 421 and 533 nm), suggesting that the electron in the first addition might be partially localized on the TA bridge linking the two porphyrins.

There is no spectral evidence suggesting reduction of either the porphyrin macrocycle or the Co(II) center in the first electron transfer process involving the TA-linked dyad, but this is not the case for the second controlled potential reduction of **6** at −1.10 V (eq 4) where the UV−visible spectrum is characterized by bands at 369, 426, and 780 nm. This spectrum resembles in part the Co(I) spectrum of $[(TPP)Co^{I}]^-$ (364 and 428 nm) or $[(P)Co^{I}]^-$ (365 and 437 nm), and it also resembles in part the product of the (PQ)Co^{II} reduction which has bands at 414, 445, and 792 nm, and is assigned as a Co(I) porphyrin with Co(II) π-anion radical character. A diagnostic near-IR band of a π-anion radical also appears in singly reduced (PQ)Co^{II} (792 nm), (QPQ)Co^{II} (814 nm), and (PQ_2)Co^{II} (750 nm), all of which also have a split Soret band (see Table 2), thus suggesting a similar electron distribution in doubly reduced **6** where one electron resides in part on each of the two cobalt centers and in part on each of the two porphyrin macrocycles. This apparent distribution of charge is consistent with **6** having the character of a molecular wire where electron density is shared throughout the molecule on both the metal center and the macrocycle.

Single Bond Linked Bis-cobalt Dyad 7. Co(PQ)-(QP)Co **7** exhibits similar electrochemical behavior as the monocobalt quinoxalinoporphyrin (PQ)Co **3**. As seen from Figures 6b and 6c, the first oxidation of **7** is 80 mV easier than for oxidation of **3**, but the second oxidations of **3** and **7** occur at identical potentials. The first $E_{1/2}$ values for the reduction of **3** and **7** are also identical, but the second reduction of **7** is easier than in **3** and is split into two peaks at −1.69 and −1.84 V, suggesting a weak interaction between the two Co(PQ) units of the doubly reduced dyad **7**.

UV−visible spectral changes obtained during the three reductions and two oxidations of Co(PQ)-(QP)Co **7** are shown in Figure 7 and Supporting Information,

(50) Le Mest, Y.; L'Her, M.; Collman, J. P.; Kim, K.; Hendricks, N. H.; Helm, S. *J. Electroanal. Chem.* **1987**, *234*, 277–295.
(51) Guilard, R.; Jerome, F.; Barbe, J.-M.; Gros, C. P.; Ou, Z.; Shao, J.; Fischer, J.; Weiss, R.; Kadish, K. M. *Inorg. Chem.* **2001**, *40*, 4856–4865.
(52) Guilard, R.; Gros, C. P.; Barbe, J.-M.; Espinosa, E.; Jerome, F.; Tabard, A.; Latour, J.-M.; Shao, J.; Ou, Z.; Kadish, K. M. *Inorg. Chem.* **2004**, *43*, 7441–7455.

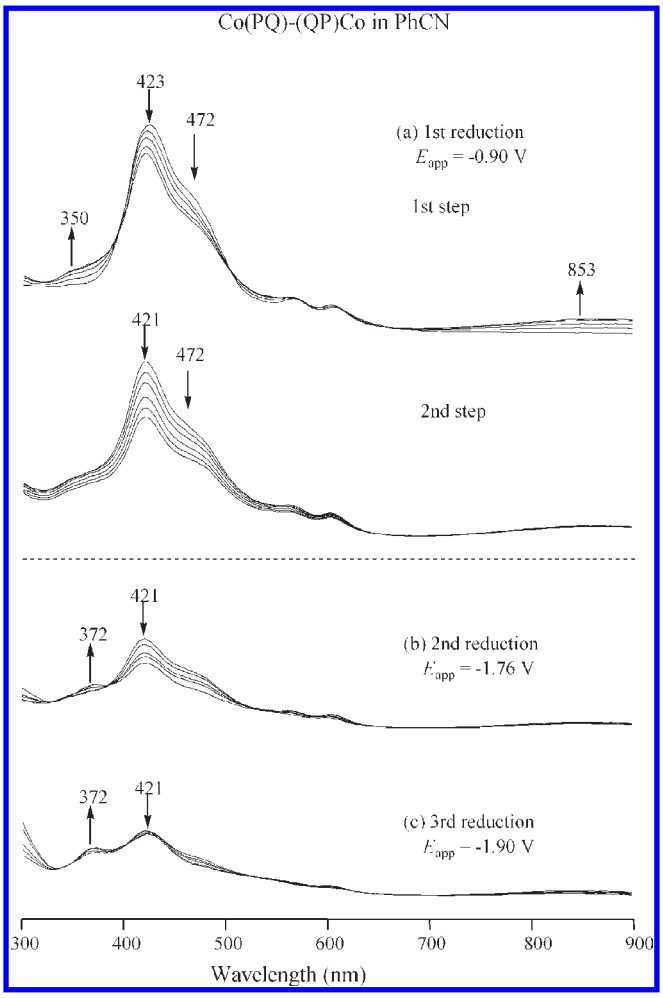

Figure 7. UV−visible spectral changes of Co^{II}(PQ)-(QP)Co^{II} **7** during reductions and oxidations in PhCN, 0.1 M TBAP.

Figure S3, respectively. Two sets of spectral changes can be observed for the first reduction at −0.90 V, consistent with two overlapped one-electron reduction processes. Comparison with the spectral changes for (PQ)Co **3** under the same solution conditions leads to a conclusion that the same redox mechanism is operative in the case of **7**.

Summary

Seven cobalt(II) and cobalt(III) porphyrins with fused quinoxaline rings at one or more β,β'-pyrrolic units of the macrocycle were synthesized and characterized as to their electrochemical properties in nonaqueous media. Each compound could be cycled between its Co(III), Co(II), and Co(I) forms under the application of a given oxidizing or reducing potential. The electrochemical and spectroelectrochemical properties of $[(P)Co^{III}]^+$, $(P)Co^{II}$, and $[(P)Co^{I}]^-$ are similar to that for the well characterized TPP derivatives in the same oxidation states. However, this is not the case for the quinoxalinoporphyrins, where the one-electron reduction of $(PQ)Co^{II}$, $(QPQ)Co^{II}$, and $(PQ_2)Co^{II}$ leads to a product with mixed Co(I) and porphyrin π-anion radical character followed by generation of a pure Co(I) π-anion radical species at more negative potentials. The position and number of quinoxaline groups on the macrocycle has little or no effect on the redox potentials for the Co(II) → Co(III) or Co(III) → Co(II) processes, but this is not the case for the other reactions where significant differences are seen between the examined compounds. Significant interactions are also observed between the two porphyrin macrocycles of the laterally bridged dicobalt(II) bis-porphyrin dyad Co(P)-TA-(P)Co in its singly and doubly reduced form, but only weak interactions is seen between the two (PQ)Co units of Co(PQ)-(QP)Co. The mixed character of the Co(I) π-anion radical is apparent in both dyad architectures and, in the case of Co(P)-TA-(P)Co, the sharing of charge between metal and macrocycle is consistent with this class of molecule being a candidate for molecular wire applications.

Acknowledgment. This work was supported by grants from the Robert A. Welch Foundation (K.M.K., Grant E-680) and the NSF of Jiangsu Province P.R. China (BK2008226). Support was also provided by a Discovery Research Grant (DP0208776) from the Australian Research Council to M.J.C.

Supporting Information Available: Figures S1−S3 illustrate thin-layer UV−visible spectral changes obtained for (QPQ)CoCl and Co(PQ)-(QP)Co during the oxidations and for (PQ_2)CoCl during the oxidation and reduction in PhCN containing 0.1 M TBAP. This material is available free of charge via the Internet at http://pubs.acs.org.